ORIGINAL RESEARCH ARTICLE

A Preterm Physiologically Based Pharmacokinetic Model. Part I: Physiological Parameters and Model Building

Khaled Abduljalil[1] · Xian Pan[1] · Amita Pansari[1] · Masoud Jamei[1] · Trevor N. Johnson[1]

Abstract

Background Developmental physiology can alter pharmacotherapy in preterm populations. Because of ethical and clinical constraints in studying this vulnerable age group, physiologically based pharmacokinetic models offer a viable alternative approach to predicting drug pharmacokinetics and pharmacodynamics in this population. However, such models require comprehensive information on the changes of anatomical, physiological and biochemical variables, where such data are not available in a single source.

Objective The objective of this study was to integrate the relevant physiological parameters required to build a physiologically based pharmacokinetic model for the preterm population.

Methods Published information on developmental preterm physiology and some drug-metabolising enzymes were collated and analysed. Equations were generated to describe the changes in parameter values during growth.

Results Data on organ size show different growth patterns that were quantified as functions of bodyweight to retain physiological variability and correlation. Protein binding data were quantified as functions of age as the body weight was not reported in the original articles. Ontogeny functions were derived for cytochrome P450 1A2, 3A4 and 2C9. Tissue composition values and how they change with age are limited.

Conclusions Despite the limitations identified in the availability of some tissue composition values, the data presented in this article provide an integrated resource of system parameters needed for building a preterm physiologically based pharmacokinetic model.

Key Points

Physiological data on the preterm population were collected and integrated from different publications.

Mathematical description of this information during development is important for building preterm physiologically based pharmacokinetic models.

Gaps in available preterm physiological data required for building an age-varying physiologically based pharmacokinetic model have been identified for future research in this area.

✉ Khaled Abduljalil
    khaled.abduljalil@certara.com

1   Simcyp Division Level 2-Acero, Certara UK Limited, 1
    Concourse Way, Sheffield S1 2BJ, UK

1 Introduction

The World Health Organization defines preterm as all births before 37 weeks of gestational age (GA) and can be subcategorised to extremely preterm (< 28 weeks of GA), very preterm (28–32 weeks of GA), and moderate-to-late preterm (32–37 weeks of GA) [1]. Worldwide, there are an estimated 15 million babies born preterm every year [2], of which, approximately 1 million die because of complications [2]. Preterm infants are exposed to various sources of injury, both in utero and after birth, at a time when their organ systems are at a critical stage of development, thus potentially causing permanent changes to their function throughout life. Many survivors face a lifetime of disability, including learning disabilities, visual and hearing problems and/or chronic diseases, such as cerebrovascular disorders, pulmonary hypertension and diabetes mellitus later in life [3]. Women who themselves were born preterm are at an increased risk of delivering their neonates prematurely [4].

Remarkable progress has been made in the clinical management of disease in preterm patients leading to an increase

in the survival rate. However, understanding the mutual impact of drugs and the developing physiology in this population is poorly understood, which in turn may translate into sub-optimal pharmacotherapy. Determining the right dose for a preterm subject is critically important. However, one of the challenges is that significant physiological 'developmental' processes occur during the neonatal period that can affect the drug kinetics or result in unpredictable exposures and/or responses to doses that are shown to be safe and efficacious in adults or older children. Another challenge is that many diseases in the preterm infant are unique, such as patent ductus arteriosus, or they may present unique manifestations, such as apnea of prematurity, owing to the anatomical and functional immaturity of various organs. These issues preclude extrapolation of dose and efficacy from adult or even older paediatric patients and require novel methods of outcome assessment, especially in infants [5, 6].

The higher extracellular fluid [7] in preterm infants compared with older children is expected to increase the distribution volume of hydrophilic drugs [8]. Conversely, the absence or lower expression of drug-metabolising enzymes and lower glomerular function contribute to lower clearance [9]. The situation is made more complex by lower concentrations of drug-binding plasma proteins compared with concentrations in older neonates [10], which can result in non-linear protein binding [11]. The underlying clinical conditions and the involvement of uptake and/or efflux transporters add another layer of complexity.

Currently, there is no widely accepted approach for the optimisation of dose in preterm neonates and whilst comprehensive clinical studies are desirable, undertaking these in preterm subjects is constrained by cost and ethical/clinical restrictions including patient recruitment and the limitations on blood sampling. Nevertheless, significant progress has been made in the field of paediatric pharmacokinetics using modelling and simulation, particularly the use of population pharmacokinetic and physiologically based pharmacokinetic (PBPK) models [12]. The PBPK models when combined with in vitro-in vivo extrapolation techniques provide a unique capability to integrate prior knowledge of anatomical, physiological and biochemical characteristics of the body together with physicochemical properties of the drug to describe various phenomena involved in the complex pharmacokinetic processes. The developed models can be used to test different scenarios and extrapolation beyond the observed data once the models and relevant parameters are qualified and verified. The PBPK approach offers a feasible alternative to empirical dosage selection where there are no clinical studies to guide the requirements [13] and has been adopted within pharmaceutical companies [14] and drug regulatory agencies [15, 16]. While the preterm PBPK model is not intended to replace clinical studies, it can facilitate making

decisions regarding first-time dosing and study design in this population.

The availability of the PBPK modelling approach can facilitate this study design process and help to explore different scenarios that can affect drug kinetics, such as a change in physiological parameters in a specific clinical condition (e.g. ductus arteriosus), presence of variants in metabolising enzymes or transporters, impact of co-medications, optimal sampling and dosing suggestions. Nonetheless, these models require comprehensive information on the magnitude of anatomical, physiological and biochemical changes during the preterm period and a reasonable knowledge of the drug disposition using in vitro information derived from human materials.

The objectives of this work are: (1) to collect data for physiological parameters that are required for building a preterm PBPK model; and (2) to incorporate system parameters as a function of individual age or/and weight within the Simcyp® Simulator to create a PBPK model that is capable of modelling altered pharmacokinetics in a preterm population. Performance of the developed PBPK-pharmacodynamic model will be explored in Part II: Applications of the Model to Predict Drugs Pharmacokinetics in Preterm Population [17].

2 Materials and Methods

2.1 Development of the Preterm Population

2.1.1 Data Sources

Demographic data on the height and weight of preterm infants born between 28 and 36 gestational weeks were obtained from the UK growth charts for the preterm population [18]. Tissue volume and composition were taken from our recently published meta-analysis [19] from 28 gestational weeks. Additional data on cardiac output, haematocrit, blood volume and binding proteins were collected from published clinical studies using, but not restricted to, MEDLINE. For each parameter, a separate search was conducted, using the keyword 'preterm or premature' plus the parameter of interest, for example 'blood volume' (see the Electronic Supplementary Material [ESM] for a full list of search terms). Article titles and abstracts were screened to maintain the focus of the search. A manual search of reference lists from relevant articles complemented the data collection process. No time period constraints were applied to the searches performed.

2.1.2 Inclusion Criteria

Data inclusion criteria were as follows: (1) individuals between 28 and 44 weeks of postmenstrual age (PMA) but within their first month of postnatal age (PNA); PMA

is calculated as the sum of GA and PNA, where PNA is the age after birth, at birth (PNA = 0) PMA equals GA. (2) Where possible, data from extreme premature neonates (GA < 28 weeks) were not included. (3) In the case of mixed-population studies, the extreme preterm individuals should not comprise more than 30% of the overall preterm sample size under study. (4) When preterm data were not available, foetal data were included. (5) Caucasian data; where Caucasian data for a specific parameter were not available, data from non-Caucasian populations were used.

2.1.3 Combining and Analysing Data from Different Studies

Whilst the majority of the data have been combined and analysed in our previous work [19], the same approach was followed to handle the additional data for blood volume, haematocrit, binding protein and cardiac output.

2.1.4 Data Analysis

Before data analysis, when a parameter was reported in different units, these units were converted to a standard unit of measurement. When the age was reported as a range, the midpoint of the interval in weeks was used. Data analysis was performed using Microsoft Excel 2013 (Microsoft Corporation, Microsoft Office Professional Plus 2013, https://products.office.com).

Meta-analyses of organ volume data and gross composition have been published earlier as a function of an individual's body weight, where longitudinal changes in systems parameters were tested using a number of commonly used growth equations, the optimal function was selected based on Akaike information criteria [19, 20]. Growth models for parameters such as plasma-binding proteins and drug-metabolising enzyme ontogeny were based on the shape of the data. For example, data that show a sigmoidal pattern suggests linear, power or exponential functions are not a likely option. For certain parameters, existing published equations were modified and used, e.g. for BSA, Meban's equation [21] and for GFR, Rhodin's equation [22], without any model discriminations. Some equations, for example, organ volume functions, were derived for the foetus that covered a wider range [19]; however, these functions are valid for the preterm population between 28 and 48 weeks PMA.

Preterm data on the height for male and female individuals were described as a function of PMA, while the preterm weight data were described as a function of both height and PMA with interaction terms to ensure that correlated demographic parameters are generated for each individual. Where original data on a parameter, such as haematocrit or protein binding, reported age as the only independent variable, growth functions of these parameters were derived based on this information. For deriving the parameter equation, the PMA was used as the independent variable, but this is only if the effect of birth on the parameter growth is minimal. However, if the parameter takes a significantly different growth rate, then PMA can no longer be used alone and another covariate should be added, which in this case was either PNA or GA.

If the preterm data were sparse or unavailable after the 37th postmenstrual week, then full-term neonatal data at birth were used. However, if the preterm data were robust, then these were used regardless of what the full-term neonatal values were at birth.

2.2 Time-Varying Physiology

Age progression in the preterm population is associated with developmental changes over time, which is expected to affect the pharmacokinetic processes. Changes in preterm individual anatomical and physiological (system) parameters during virtual simulations are very relevant to this population when simulating long-term infusions or multiple doses over a few days, where the system parameters are changing rapidly over a relatively short time, i.e. on a daily basis or within a week. Paediatric PBPK models are inherently suited for this task as the whole physiology can be updated during the time course of a simulation. To ensure that the covariates are growing while the simulation is progressing, a time-dependent updating scheme is required for covariates. Details of this approach have been previously published and applied to full-term newborn subjects [23], these features were also incorporated for the preterm population.

3 Results

3.1 Population Parameters

3.1.1 Demographics

3.1.1.1 Age Distribution The preterm PBPK model was developed for preterm individuals with a PMA between 28 and 40 weeks at birth until they reach their 44th week PMA (i.e. 0.538 and 0.850 year). The assumption here is that after 44 weeks PMA, the system parameters for preterm neonates behave like those of 1-month full-term neonates, i.e. the impact of prematurity is diminishing. Apart from body weight, longitudinal preterm studies for organ weight and blood flow showing differences from full term are not available.

3.1.1.2 Height The following equations were derived based on UK growth charts for both male and female individuals [18] to describe the subject height per sex for a preterm population (Fig. 1):

$$\text{Male height (cm)} = -43.205 \times \text{PMA}^2 + 111.84 \times \text{PMA} - 9.4871,$$

$$\text{Female height (cm)} = -50.927 \times \text{PMA}^2 + 121.53 \times \text{PMA} - 13.304,$$

where PMA is the post-menstrual age in years.

3.1.1.3 Body Weight Preterm data on total body weight at different PMAs were obtained from UK growth charts for both male and female individuals [18]. The following equations were derived based on these datasets to describe weight per sex based on height and PMA for the preterm population (Fig. 2):

$$\text{Male weight (kg)} = \text{PMA} \times (0.0373 \times \text{HT})^{2.36},$$

$$\text{Female weight (kg)} = \text{PMA} \times (0.0375 \times \text{HT})^{2.31},$$

where PMA is the postmenstrual age in years and *HT* is the individual height in centimetres, predicted using the given equations above.

Because the individual height and PMA for male and female individuals were used to describe the body weight, no residual random variability was required to describe interindividual variability in the latter (i.e., the random uncorrelated variability for both sexes weight is zero). Determining weight based on height ensures a correlated Monte-Carlo approach with realistic weight per body height [24].

3.1.1.4 Body Surface Area The BSA was calculated based on a modified version of Meban's equation [21], which was based on weight in grams (hence the coefficient was updated) and height. Here, the predicted height and weight were used to calculate the BSA as below:

$$\text{BSA (m}^2) = 0.0315 \times \text{WT}^{0.562} \times \text{HT}^{0.320},$$

where WT is the predicted individual body weight in kg and HT is the predicted individual body height in centimetres. The equation is the same for both male and female preterm populations. Performance of this equation was checked against observed data [21, 25, 26] and presented in Fig. 3 (the Haycock equation was used to generate BSA data for comparison).

3.1.2 Body Gross Composition

Preterm physiological body composition, including total water, extra- and intracellular water, fat and fat-free mass determine the drug volume of distribution in preterm populations.
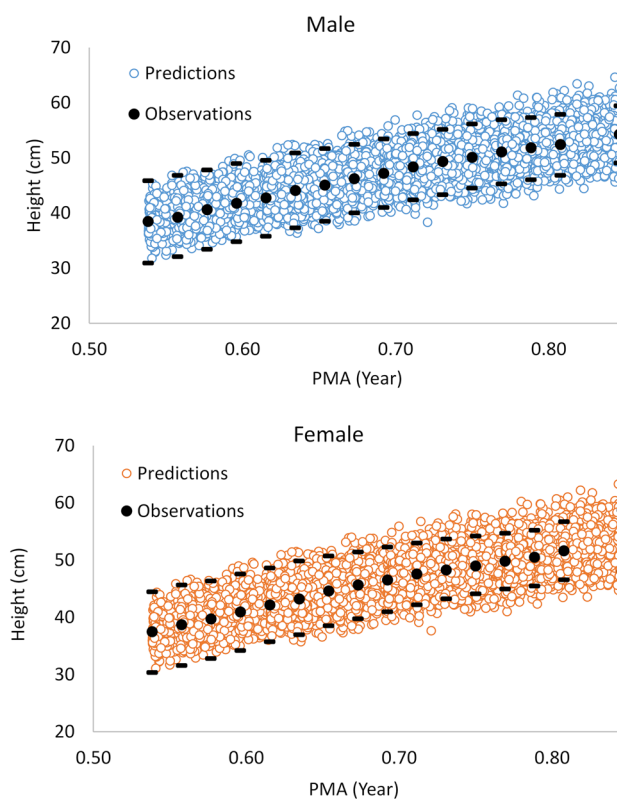

Fig. 1 Preterm height (cm) as a function of PMA (years) for male (top) and female (bottom) subjects. Black filled circles are observations from UK growth charts [18], dashed black lines represent the 0.4% and 99.6% percentiles for the observed data. Coloured open circles represent physiologically based pharmacokinetic model predictions using the sex-based height equations. A variability [coefficient of variation (CV%)] of 6% for both sexes was required to recover observed inter-individual variability in body height between 0.4 and 99.6% percentiles

3.1.2.1 Body Water A previous meta-analysis of the collected data indicated that the total body water increases from 0.358 ± 0.054 to 0.863 ± 0.151, 1.530 ± 0.240, 2.215 ± 0.265 and 2.588 ± 0.241 L at 23, 27, 32, 37 and 40 PMA (in weeks), respectively. The intracellular water (percentage of body weight) increases from 22.8 ± 3.4 to 24.8 ± 3.7, 26.7 ± 4.0, 28.7 ± 4.3 and $29.9 \pm 4.5\%$ at 23, 27, 32, 37 and 40 PMA (in weeks), respectively. In contrast, the extracellular water (percentage of body weight) decreases from 61.7 ± 3.7 to 57.2 ± 4.5, 51.6 ± 5.4, 45.6 ± 6.1 and $41.9 \pm 6.2\%$ at 23, 27, 32, 37 and 40 gestational weeks, respectively. The corresponding average body weights at these ages are 0.42, 1.1, 2, 3 and 3.6 kg, respectively [20]. The following equations were derived to describe the changes in total, intracellular and extracellular water during growth for both male and female subjects:

$$\text{Total body water (L)} = 0.862 \times \text{WT} - 0.04 \times \text{WT}^2,$$

$$\text{Intracellular water (L)} = 10 \times \text{WT} \times (0.015 + 0.018 \times \text{PMA}),$$
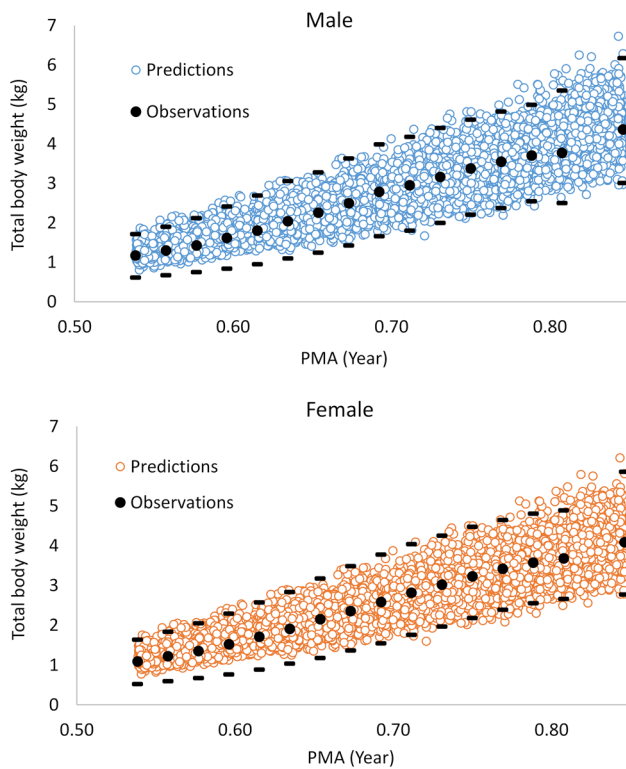
Fig. 2 Preterm body weight (kg) as a function of postmenstrual age (PMA, years) for male (top) and female (bottom) subjects. Black filled circles are observations from UK growth charts [18], dashed black lines represent the 0.4% and 99.6% percentiles for the observed data. Coloured open circles represent physiologically based pharmacokinetic (PBPK) model predictions using the sex-based weight equations. Propagated variability from individual height was sufficient to recover observed inter-individual variability in body weight between the 0.4 and 99.6 percentiles. No additional variability was required for weight equations to match the observed data
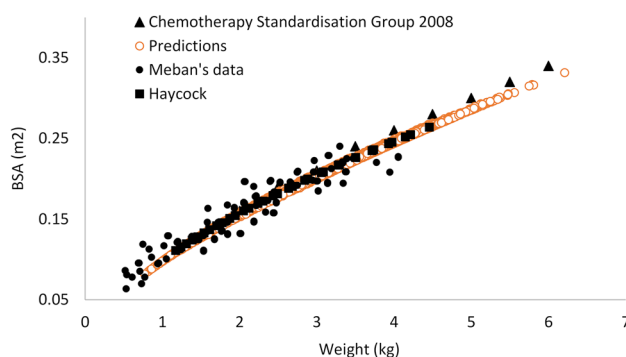

Fig. 3 Predicted body surface area (BSA, m^2) in the preterm population (coloured open circles). Observations from different clinical resources are given as black filled circles (Meban [21]), black filled triangles (Chemotherapy Standardisation Group [26]) and black filled squares (Haycock et al. [25])

Extracellular water (L) = total body water − intracellular water, where WT is the neonatal body weight in kilograms and PMA is the postmenstrual age in years. Performance of these equations together with observed values [27–31] are given in Fig. 4. The propagated variability from total body weight seems sufficient to recover the observed inter-individual variability for total and extracellular water in preterm neonates. Intracellular water is expected to be less variable. However, the magnitude of variability in this parameter is unknown in the preterm population.

3.1.2.2 Body Fat and Fat-Free Mass A previous meta-analysis of the collected data on body fat and fat-free mass indicated that the total body fat-free mass (mean ± standard deviation) increases from 0.42 ± 0.06 to 1.01 ± 0.18, 1.81 ± 0.29, 2.66 ± 0.34 and 3.15 ± 0.32 kg at 23, 27, 32, 37 and 40 PMA (in weeks), respectively. The corresponding total body weights are 0.42, 1.1, 2.0, 3.0 and 3.6 kg, respectively. The total body fat mass (mean ± standard deviation) increases from 0.008 ± 0.003 to 0.04 ± 0.02, 0.14 ± 0.05, 0.32 ± 0.10 and 0.50 ± 0.11 kg at 23, 27, 32, 37 and 40 PMA (in weeks), respectively. The corresponding total body weights are 0.42, 1.0, 2, 3.0 and 3.6 kg, respectively [20]. The following equations determine the fat mass and fat-free mass for both male and female subjects:

Fat mass, $FM \, (kg) = (0.185 \times WT)^{1.9}$,

Fat-free mass, $FFM \, (kg) = WT - FM$,

where WT is the neonatal body weight in kilograms. The performances of these equations together with observations [29, 30, 32–39] are given in Fig. 5. The propagated variability from total body weight seems sufficient to recover the observed inter-individual variability for fat mass and fat-free mass in preterm neonates.

3.2 Haematocrit

Preterm haematocrit is described using the following derived equation based on published data [40–43] presented in Fig. 6. The equation is applied to both male and female preterm subjects:

$Hct \, (\%) = 28.59 + 0.592 \times GA - 3.982 \times PNA$,

where GA and PNA are the individual gestational age and postnatal age in weeks, respectively. To recover the observed variability, a residual random effect of 15% (average coefficient of variation [%CV] from the meta-analysis) across preterm age was applied.
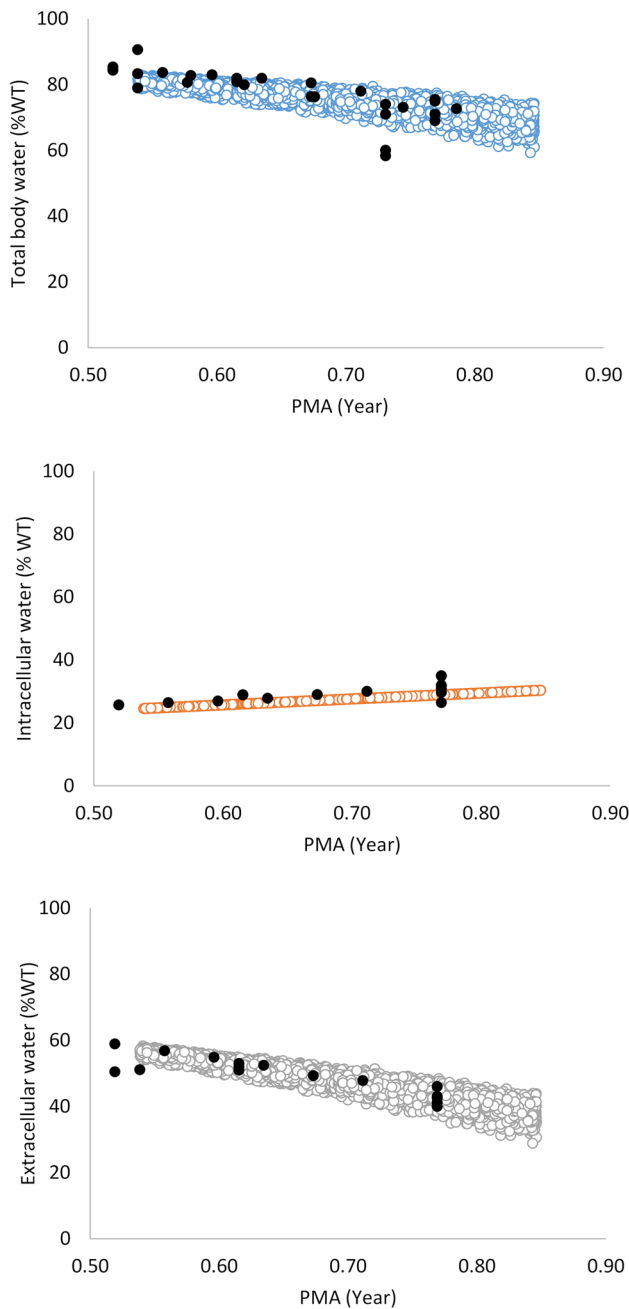
Fig. 4 Body water (% body weight) during growth. Black filled circles are observations (see text) and coloured open circles are predictions for preterm neonates
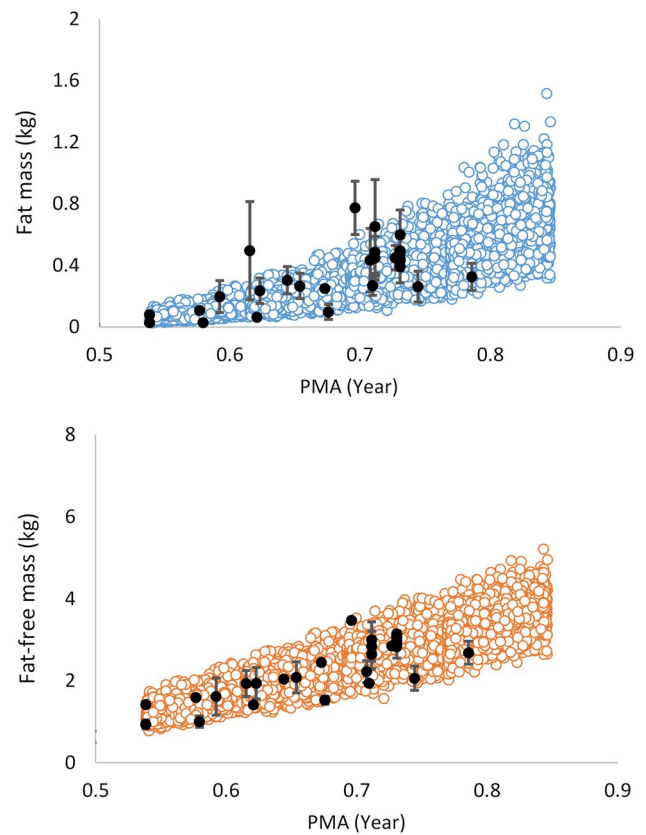

Fig. 5 Neonatal body fat and fat-free mass during growth. Black filled circles are observations (see text) and error bars represent the standard deviation; the coloured open circles are predictions for preterm neonates

$$\text{Blood volume (L)} = 0.083 \times \text{WT},$$

where WT is the total body weight in kilograms.

The plasma volume in male and female preterm subjects was calculated from blood volume and haematocrit according to the following function:

$$\text{Plasma volume (L)} = (1 - \text{Haematocrit} \times 0.91) \times \text{Blood volume},$$

where 0.91 is the body/venous haematocrit ratio [48].

Red blood cells volume can be calculated as the difference between blood and plasma volumes in both sexes using the following equation:

$$\text{RBCs volume (L)} = \text{Blood volume} - \text{Plasma volume}.$$

3.3 Blood, Plasma and Red Blood Cell Volumes

The preterm blood volume was the average value for reported blood volume of 85 [44], 83 [45], 79.1 [46] and 84.7 [47] mL/kg of body weight, yielding a mean blood volume value of 83 mL/kg. Hence, the following equation was applied to both male and female preterm subjects:

3.4 Protein Binding

Changes in the unbound fraction (fu) of drugs in the plasma of preterm subjects (fu_{Preterm}) were estimated using the following equation [49]:

$$fu_{\text{Preterm}} = \cfrac{1}{1 + \cfrac{(1 - fu_{\text{Adult}}) \times P_{\text{Preterm}}}{fu_{\text{Adult}} \times P_{\text{Adult}}}},$$

Fig. 6 Preterm haematocrit (%) during development. Coloured filled circles are observations and error bars represent the standard deviation (SD). Dashed lines represent upper and lower SDs predicted using an additional 15% coefficient of variation (%CV)
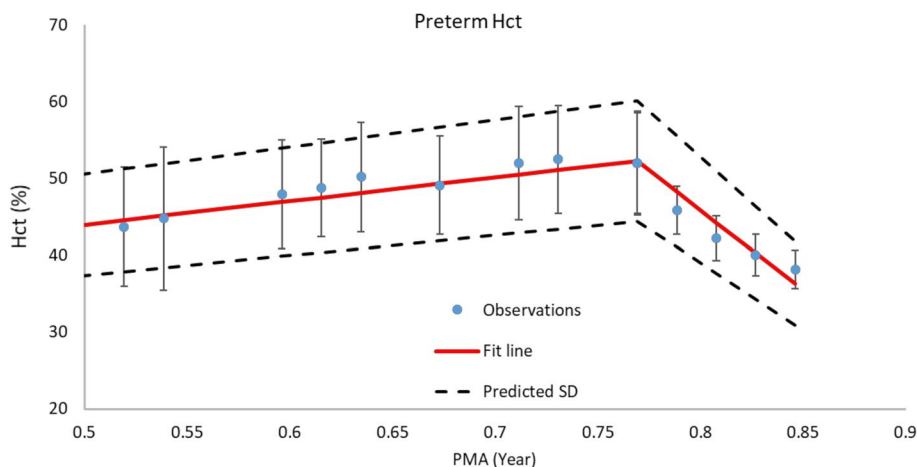
where P is the plasma protein concentration (serum albumin or alpha 1 acid-glycoprotein) and fu_{Adult} is the average unbound fraction of drug in healthy adults. Note that the P unit can be either g/L or μM as these units cancel out in the equation.

3.4.1 Human Serum Albumin

A meta-analysis of published data on plasma albumin levels [51–54] suggested that the average value increased from 29.52 g/L at 28 weeks of PMA (i.e. 0.538 years) to 31.69, 34.34, 35.51, 36.44 and 36.95 g/L at 31, 36, 39, 42 and 44 weeks of PMA, respectively. Dividing the PMA by 52 weeks to give a value in years and fitting the meta-analysed data (Fig. 7) suggested that the preterm albumin can be described by the following function (for both sexes):

$$\text{Plasma Albumin} \, (\text{g/L} \,) = \frac{41.3 \times \text{PMA}^{2.70}}{0.383^{2.70} + \text{PMA}^{2.70}},$$

where PMA is the postmenstrual age in years. A CV of 10% was added to the predicted values to cover the observed inter-individual variability in this parameter.

3.4.2 Alpha 1 Acid-Glycoprotein

A meta-analysis of published data on preterm alpha 1 acid-glycoprotein plasma levels [19, 51, 56–57] suggested that the average value increased from 0.01 g/L at about 25 weeks of PMA to 0.03, 0.12, 0.32, 0.43 and 0.58 g/L at 29, 35, 40, 42 and 44 weeks of PMA, respectively. Dividing the PMA by 52 weeks and fitting the meta-analysed data (Fig. 8) suggested that the preterm alpha 1 acid-glycoprotein can be described by the following function (for both sexes):

$$\text{Alpha-1 acid glycoprotein} (\text{g/L}) = 0.0013 \times e^{(7.12 \times \text{PMA})},$$

where PMA is the postmenstrual age in years. A CV of 13% was added to the predicted values to cover the observed inter-individual variability in this parameter.

3.5 Tissue Volumes

Tissue volume parameters are required for the PBPK model to allow prediction of drug distribution to different tissues and hence prediction of individual tissue exposure over time. Information on tissue volumes for the preterm population were derived based on published meta-analyses [19] across a wide GA range. Data applied to the preterm have been given in the ESM. The following equations determine the tissue volumes based on the total body weight (WT), in kilograms, for both male and female preterm subjects:

$$\text{Adipose volume} \, (\text{L}) = (0.2586 \times \text{WT})^{1.91}$$

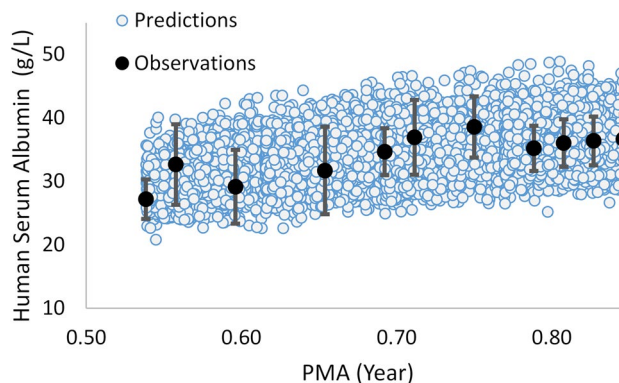$$\text{Heart volume} \, (\text{L}) = \frac{(0.0047 \times \text{WT})^{0.91}}{1.04}$$

Fig. 7 Preterm serum albumin level comparing the predicted and observed values. Coloured open circles are the predictions and black filled circles are the observations with error bars representing the standard deviation

Fig. 8 Preterm alpha-1 acid-glycoprotein level comparing the predicted and observed values. Coloured open circles are the predictions and black filled circles are the observations with error bars representing the standard deviation
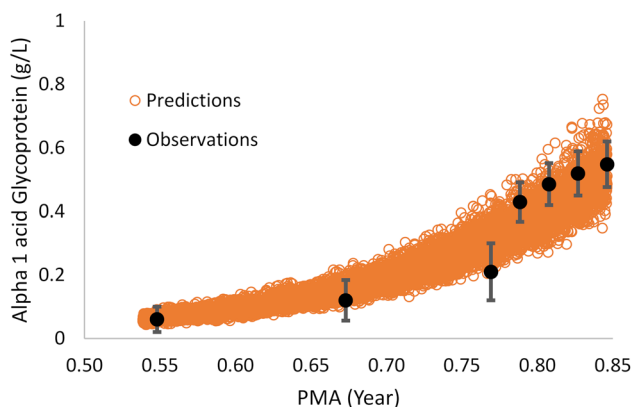
$$\text{Brain volume (L)} = \frac{(0.116 \times \text{WT})^{0.915}}{1.04}$$

$$\text{Liver volume (L)} = \frac{(0.0036 \times \text{WT})^{0.925}}{1.08}$$

$$\text{(both) Kidneys volume (L)} = \frac{(0.0054 \times \text{WT})^{0.88}}{1.035}$$

$$\text{Pancreas volume (L)} = \frac{(0.0009 \times \text{WT})^{0.91}}{1.045}$$

$$\text{Muscle volume (L)} = \frac{(0.251 \times \text{WT})^{1.46}}{1.04}$$

$$\text{Skin volume (L)} = \frac{(0.1005 \times \text{WT})^{1.2}}{1.1}$$

$$\text{(Both) Lungs volume (L)} = \frac{(0.0077 \times \text{WT})^{0.762}}{1.05}$$

$$\text{Spleen Mass (kg)} = \frac{(0.0068 \times \text{WT})^{1.18}}{1.06}$$

$$\text{Bone volume (L)} = \frac{(0.0294 \times \text{WT})}{1.65}$$

Gastrointestinal tract volume (L)

$$= (0.0024 + 0.0109 \times \text{WT} + 0.0048 \times \text{WT}^2)/1.04.$$

The propagated variability from total body weight seems sufficient to recover the observed inter-individual variability for each tissue (see figures in the ESM). Developmental

changes of organ volumes for a representative male preterm subject are shown in Fig. 9.

3.6 Tissue Composition

Information on tissue composition provide key parameters determining the drug partition into different tissues. Models are available to predict the partition ratio between each tissue and plasma based on the tissue compositions [58–60]. Collected data on percentages of lipids and water in premature tissues required for the PBPK distribution model are given in Table 1. Because of the lack of some information, the following assumptions were made:

(a) The acidic phospholipids (mg/g of tissue) and tissue-to-plasma ratios for binding proteins (albumin and lipoprotein) in the preterm infant are similar to the adult.

(b) For each tissue, the fractional volumes (as percentages) of extracellular and intracellular water, neutral lipids and neutral phospholipids in the preterm infant are the same as those percentages in the full-term paediatric individuals at birth (40 GA).

Because these tissue composition values are relative to the tissue size, which is age dependent, the absolute values for tissue composition are age dependent.

3.7 Cardiac Output and Blood Flow

3.7.1 Cardiac Output

Data on cardiac output in preterm subjects between 27 and 40 GA (both male and female) were collated from the literature [70–87] (see the ESM). These studies reported the results after normalising per kilogram of body weight without explaining the percentage of variability from this covariate. In the case of patients with patent ductus arteriosus, the average value of both left and right ventricle output was used. These data can be described using the following function:

Cardiac output (L/h) = $12 \times \text{WT}$,

where WT is the preterm total weight in kilograms. No additional variability was added to the predicted values as the physiological variability coming from body weight was adequate to meet the observed variability. A comparison between the predicted and observed cardiac output is shown in Fig. 10.
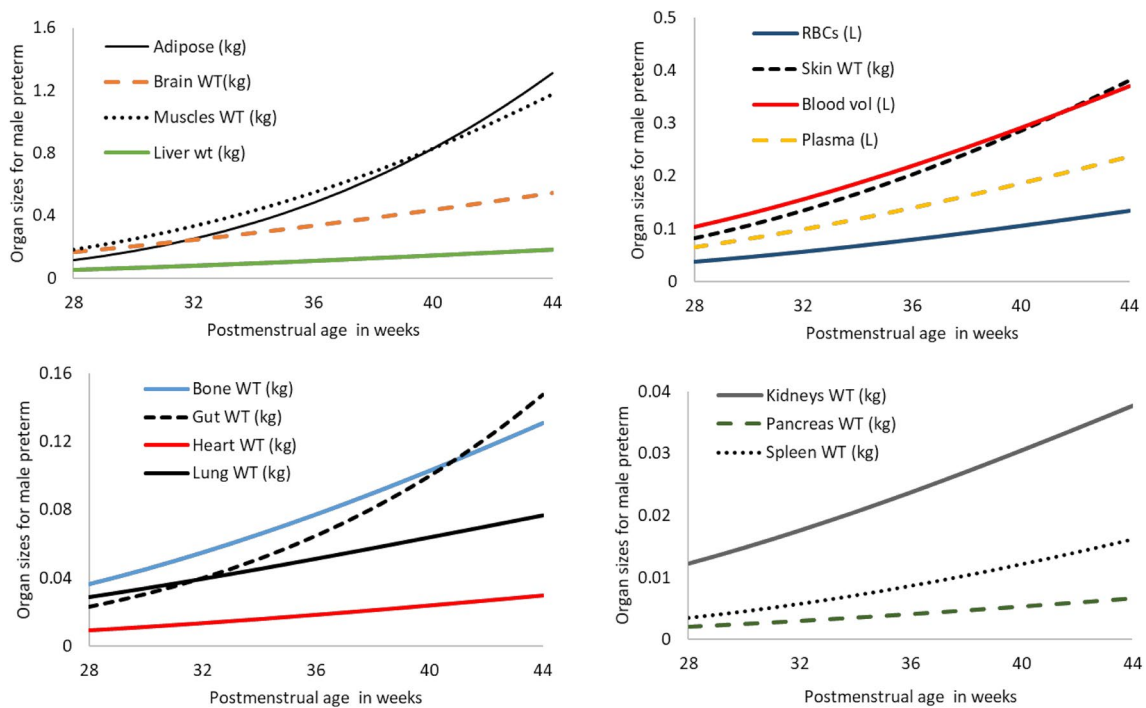
Fig. 9 Tissue sizes for a representative preterm male subject during development from 28 to 44 postmenstrual weeks. Predictions of individual tissue size vs. observations are given in the Electronic Supplementary Material

Table 1 Preterm tissue composition

Organ	% of Tissue mass			
	Water	References	Total lipids	References
Adipose	59.7	[61]	34.7	[61]
Bone	$72.368 - 0.2032 \times PMA$	[62] and full term	$0.0062 \times PMA - 0.0578$	[62] and full term
Brain	$86.767 + 0.3861 \times PMA$ $- 0.0081 \times PMA^2$	[63, 64] and full term	$1.9896 + 0.036 \times PMA$	[63] and full term
Gut	79.493	Full term	2.500	Full term
Heart	$88.137 - 0.0901 \times PMA$	[61, 65, 66]	$1.6071 + 0.0136 \times PMA$	[61, 65, 66]
Kidney	$94.654 - 0.2699 \times PMA$	[66] and full term	2.73	Full term
Liver	$85.315 - 0.1477 \times PMA$	[66, 67] and full term	2.4	[61]
Lung	86.117	Full term	3.1	Full term
Muscles	$98.229 - 0.4004 \times PMA$	[61, 63, 68, 69]	2	[61]
Pancreas	78.4	Adult	5.03	Adult
Plasma	96.0	Full term	0.393	Full term
RBC	66.6	Full term	0.46	Full term
Skin	84.38	Full term	Adult	Adult
Spleen	83.8	[61]	1.5	[61]

PMA postmenstrual age, *RBC* red blood cell

3.7.2 Tissue Blood Flow

Because of limited information regarding the individual tissue blood flows in preterm neonates, the same percentages of cardiac output for full-term neonates was assumed.

The absolute blood flow to each tissue is PMA dependent because the preterm cardiac output varies with this parameter. The tissue blood flows for male and female individuals are given in Table 2.

3.8 Renal Function

Glomerular filtration rate (GFR) in preterm subjects has been extensively reviewed in the past, a function based on the individual's PMA, and body weight has been published [22]. The preterm GFR function within the Simcyp Simulator to describe drug filtration renal clearance was a modification of Rhodin et al.'s equation [22]:

$$\text{GFR}\left(\frac{\text{mL}}{\text{min}}\right) = 121 \times \left(\frac{\text{PMA}^{3.4}}{0.923^{3.4} + \text{PMA}^{3.4}}\right) \times \left(\frac{\text{WT}}{70}\right)^{0.75},$$

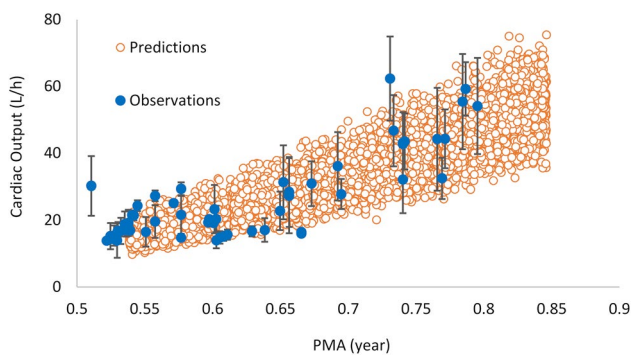where PMA is the postmenstrual age in years, and WT is the total body weight in kilograms for a preterm subject.

Fig. 10 Comparison of the predicted and observed cardiac outputs in the preterm population. The blue filled circles are the observed data and the error bars represent the standard deviation. The predicted values are shown using brown open circles. Note the observed data here were corrected to the mean bodyweight reported in the original publications as individual data were not available

The preterm GFR was found to be affected by the process of birth for preterm subjects [88] and because of collinearity in the weight and GA for preterm subjects, it can equally be described by PMA and GA. However, the inter-individual variability in the latter case is too narrow to describe the clinical observed variability in preterm GFR, whilst by using body weight and PMA, sufficient physiological variability is generated to attain the observed variability.

3.9 Metabolism

3.9.1 Development of 'First-Pass' Gut Metabolism

The gut metabolism of cytochrome P450 (CYP) substrates in the small bowel was assumed to be dependent on gut surface area and the abundance of CYPs. Intestinal length and diameter were both related linearly to BSA [12]. First duodenal length was calculated based on clinical measurements and by mapping age with BSA [89, 90]. Similarly, the jejuno-ileal length was calculated based on BSA using published measurements [90, 91]. The following equations were derived:

$$\text{Duodenal length (m)} = 0.139 \times \text{BSA}^{0.569},$$

$$\text{Jejuno-ileal length (m)} = 7.05 \times \text{BSA}^{0.633}.$$

Total intestinal length was calculated as the sum of values from these equations. A fixed assumed CV of 20% was added to the jejuno–ileal length to achieve the observed variability in the intestinal length.

For the intestinal diameter, the duodenal diameter was calculated based on published measurements in the duodenal

Table 2 Tissue blood flow in preterm populations

Tissue	Blood flow (% of cardiac) output		References
	Male	Female	
Adipose	5	5	Assuming full-term paediatric value
Lung	100	100	Assuming full-term paediatric value
Skin	5	5	Assuming full-term paediatric value
Kidneys	16	16	[83]
Brain	10	10	[79]
Muscle	6.03	6.03	Assuming full-term paediatric value
Bone	5	5	Assuming full-term paediatric value
Stomach and oesophagus	1	1	Assuming full-term paediatric value
Small intestine	10	11	Assuming full-term paediatric value
Large intestine	4	5	Assuming full-term paediatric value
Spleen	2	3	Assuming full-term paediatric value
Pancreas	1	1	Assuming full-term paediatric value
Liver (artery + portal[a])	25.5 (6.5 + 19.0)	28 (6.5 + 21.5)	Assuming full term paediatric value
Heart	4	5	Assuming full term paediatric value

[a]Pancreas, spleen and gut (stomach and oesophagus plus small intestine plus large intestine) are part of the liver portal vein blood flow

at four different sites at each gestational week between 22 and 40 weeks. The average of these four site measurements at each GA was used [89] and related to individual BSA generated using the BSA equation given earlier.

$$\text{Duodenal diameter (m)} = 0.021 \times \text{BSA}^{0.651}.$$

The jejunal and ileal diameters were calculated as a proportion of the diameter of the duodenum (0.9 and 0.8 for the jejunum and ileum, respectively). A fixed assumed CV of 20% was added to achieve the observed intestinal diameter variability. Age-related changes in duodenal, jejunal and ileal surface areas were calculated from the corresponding lengths and diameters incorporating the calculated variability. The model assumes that both the stomach and colon do not contribute to the drug absorption, but they do contribute to the drug distribution and they are part of the gastrointestinal organ in the distribution model.

Limited data exist on the intestinal expression of metabolising enzymes in preterm neonates. Cytochrome P450 3A4 expression was practically absent with no activity in 11 foetal duodenal samples (9–15 GA) and was expressed at around 40% of adult levels in six full-term neonates aged 2–4 weeks [92]. Another study only detected CYP3A protein in 50% of samples for individuals aged 1–6 months with no correlation between CYP3A4 protein and messenger RNA [93]. The CYP3A4 and CYP3A5 messenger RNA levels were in the same order of magnitude. Cytochrome P450 3A7 messenger RNA expression was much lower and only detected in 64% of the duodenal samples and did not vary with age, suggesting that the contribution of this enzyme to enterocytic metabolism is very limited [93].

In conclusion, the intestinal metabolism due to CYP enzymes in preterm subjects is expected to be very low owing to lower enzyme expression per volume of enterocytes and a smaller gut size compared to adults. Therefore, intestinal metabolism was not taken into account in the current model; however, it can be incorporated if ontogeny functions for intestinal enzymes are known.

3.9.2 Hepatic Metabolism

Preterm hepatic metabolism is calculated similarly to that of a full-term paediatric subject [12], where the enzyme maturation function (i.e. ontogeny) is multiplied by the adult value for each enzyme abundance distribution:

$$\text{Enzyme i Abundance}_{\text{preterm}} = \text{Enzyme i Abundance}_{\text{adult}} \times \text{Ontogeny Function},$$

where the adult variability around the mean abundance value for enzyme i is applied to the enzyme abundance in preterm. Clearance is then scaled according to the method described elsewhere [94]. A similar approach is applied to

the transporter models allowing investigation of transporter effects on the pharmacokinetics and pharmacodynamics in the preterm population.

3.9.3 Ontogeny

Information on hepatic CYP ontogeny functions in preterm subjects was obtained from the literature and discussed under the relevant enzyme below. Limited studies investigated the changes in CYP-metabolising enzymes in preterm subjects. Among CYPs, there were only data showing a developmental pattern for CYP1A2, CYP2C9 and CYP3A4 with PMA (Fig. 11). No clear trend of ontogeny for CYP3A7, CYP2D6 and CYP2C19 was found.

3.9.3.1 CYP3A4
Cytochrome P450 3A4 ontogeny function (Fig. 11) is described as a linear function of PMA based on the in vitro expression and activity data in foetal and neonatal liver microsomes [95–97]:

$$\text{CYP3A4 (Fraction of adult)} = 0.003 + 0.1331 \times \text{PMA},$$

where PMA is in years.

3.9.3.2 CYP1A2
Ontogeny profiles (Fig. 11) based on functional activity have been derived for the hepatic CYP1A2 using deconvoluted in vivo clearance data [98]. This ontogeny function was modified for the preterm population of 28–44 weeks (0.54–0.855 year) PMA is described as a power function:

$$\text{CYP1A2 (Fraction of adult)} = 0.81 \times \text{PMA}^{5.2},$$

where PMA is in years.

3.9.3.3 CYP2C9
The ontogeny function (Fig. 11) for the hepatic CYP2C9 was derived based on abundance values obtained using western blotting for individuals aged between 28 and 44 weeks of their PMA (0.54–0.855 year) [99]. The derived function is given below:
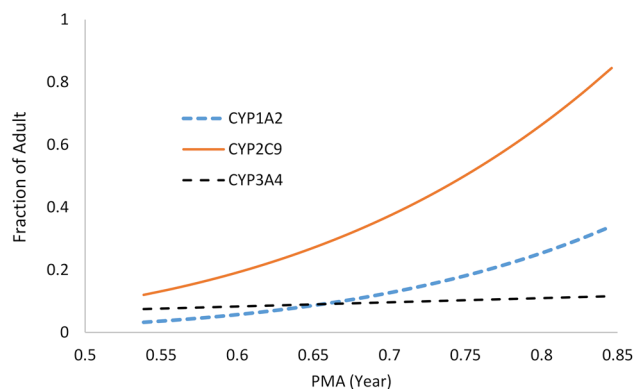

Fig. 11 Ontogeny profiles for cytochrome P450 (CYP) 1A2, 2C9 and 3A4 in the preterm population

CYP2C9 (Fraction of adult) $= 1.74 \times \text{PMA}^{4.32}$,

where PMA is in years.

3.9.3.4 CYP3A7 The hepatic CYP3A7 is known to be over-expressed in the foetus and its level decreases with GA, but there is no consensus on its activity [95] and/or the expression [96, 97] measurements. In one study, the CYP3A7 activity relative to adult was about nine-fold higher in 26 foetuses < 30 weeks of GA and decreased to six fold of adult in eight foetuses over 30 weeks of GA. Within 24 h of birth in two preterm neonates, born at 30 ± 3.5 weeks of GA, the activity was 12-fold of adult with a peak of 15.7-fold of adult in ten preterm children (32.4 ± 4.5 weeks of GA) during their first week of life. The activity then fell to 6.7-fold in eight preterm neonates (34.2 ± 5.4 weeks of GA) during their first 8–28 days of life [95]. In a later study, the expression of CYP3A7 was approximately 27-fold of adult in the foetuses between 13 and 24 weeks of GA and declined to 17-fold of adult at the aged of 31–41 weeks of GA. A further decrease to 8.7-fold of adult was reported after birth within 3 months [96]. These results are in better agreement with another study showing that between 27 and 40 weeks of GA the expression is about 17-fold higher than adults and decreases to about 12-fold of adult during the first 0–29 days of life [97].

3.9.3.5 CYP2D6 The hepatic CYP2D6 protein expression was found to be about 2% of the adult level for extensive metaboliser phenotypes within 24 h after birth from preterm samples born at 29 weeks of GA, this level increased to 14% within 1–7 days after birth (33.8 weeks of GA) and further increased to 28% within 7–28 days after birth at 31.5 weeks of GA [100]. In the same study, the reported activity was about 2% of adult within 24 hours in the preterm group and increased to 9% during the first 1–7 days and 25% of adult within the first 7–28 days of birth [100]. In contrast, another study found large inter-individual variability in the liver samples with an average activity of 26% and 28% of adult during 26–40 weeks of GA and 0–7 days after birth with no relationship with the individuals' genotype. This activity level increased to 47% after 7 days and remained around this level till 18 years of age [101]. This is unexpected as the reported median activity for the > 7 days to 18 years age group was 0.033 nmol/min/mg of protein, which is considerably lower than the activity determined for a pooled adult human liver microsomal sample (0.168 nmol/min/mg). Nevertheless, the original study found a correlation between CYP2D6 activity and protein in individual tissue.

3.9.3.6 CYP2C19 The protein expression of hepatic CYP2C19 (and activity data using mephenytoin) suggested that CYP2C19 expression (15% of adult at birth) did not change during the second and third trimesters and even

1 month after birth, there was high inter-individual variability [99].

4 Discussion

Physiological parameters required to build preterm PBPK population models have been collated and equations derived to describe their change (mean and the associated variability) during development. Equations were integrated within a PBPK model and verified for their inter-individual variability within physiological ranges down to 28 GW.

The preterm model was built using UK growth charts and thus represents a Caucasian population. The integrated preterm PBPK model was built with flexibility to incorporate information from other ethnic groups if needed, i.e. growth chart or other physiological information from a Japanese preterm population.

Available information on organ volumes required for building a PBPK model for the preterm population in age- and/or weight-dependent functions has been collected from different sources and quantified in the current work. Preterm ontogeny functions have been developed for three major hepatic enzymes, namely, CYP3A4, CYP1A2 and CYP2C9. However, for other enzymes such as CYP3A7, CYP2D6 and CYP2C19, the available information did not show a definitive change with PMA. The PBPK model framework allows the incorporation of specific ontogeny functions to explore various ontogeny patterns necessary to recover clinical data. The development of 'in vivo' ontogeny profiles may allow better prediction of observed data within such models [98].

The age-dependent function of drug-binding protein in plasma was also included in the population database. The lower protein-binding level in the preterm population compared with older neonates can affect the disposition of drugs [10]. Cardiac output is another parameter with high variability owing to the fact that this population has different underlying conditions (pulmonary distress, ductus arteriosus, infections).

Recent efforts have been made to build a PBPK model for the preterm population. Claassen et al. published a preterm PBPK model without providing information on growth functions for all organs and their inter-individual variability, nor how changes to binding proteins and haematocrit were accounted for. Interestingly, the blood flow for major organs such as muscle, fat and bone were not shown; however, the flow to different gut segments was presented, while the only considered route of administration in the model was intravenous [102]. The model performance was verified using amikacin and acetaminophen. More recently, Yang et al. published a PBPK model for term and preterm neonates and infants that was built in R for seven tissues, namely liver, fat, brain, muscle kidney, blood and the rest of the body as well

as the GFR maturation [103]. This paper did not consider the gut or lung, which is important in the preterm PBPK model, nor did it mention physiological parameters affecting absorption or ontogeny of enzymes involved in metabolism. In contrast to Claassen et al.'s model, Yang et al.'s model provided detailed methodology including model equations for physiological parameters and the associated variability; however, performance of the model in the prediction of preterm pharmacokinetics was lacking

A major drawback of the available data is the lack of longitudinal investigation of system parameters and the high variability in the available cross-sectional studies in this special population. Anatomical and physiological parameter equations have been added to the Simcyp Simulator with the ability to modify the equations parameters and structures of the equations if required using the same approach as already mentioned for CYPs. Thus, fixed parameters based on full-term neonatal values, such as fractions of blood flow to some organs and tissue composition, can be modified in the light of any new data as they become available on for instance PMA-, PNA- or GW-related changes or changes in specific disease states.

The developed stochastic preterm PBPK model aims to predict pharmacokinetics in preterm subjects. The model also allows the incorporation of the growth of physiological parameters during simulations. Allowing these covariates, i.e. physiological parameters to grow while simulation progresses to reflect the realistic and dynamic nature of drug disposition is a feature that has been shown to be relevant to full-term neonates [23].

Because of the diversity of pathophysiological conditions and developmental changes, pharmacokinetic investigation in a preterm population is challenging. Current modelling tools that support data analysis for the preterm population are to a large extent limited to a traditional pharmacokinetic analysis with a clear shift towards population pharmacokinetics to make use of sparse data normally collected for this population. The PBPK approach allows extrapolation and exploring 'what if' scenarios provided the drug's absorption, distribution, metabolism, and excretion is well characterised and information on physiological changes that could affect the absorption, distribution, metabolism, and excretion of the drug are considered [104]. Another advantage of the PBPK model is the use of sensitivity analysis to explore 'what if' scenarios, for example, the effect of haemodynamic changes due to ductus arteriosus on drug kinetics or the effect of the suppression of drug-metabolising enzymes in respiratory distressed preterm subjects on drug clearance. The preterm population model is flexible and allows the changing of physiological parameters to mimic different disease conditions.

While the drug parameters can be investigated experimentally, the systems parameters are multidimensional with time-varying changes to plasma protein binding, cardiac output, drug metabolism and renal function occurring simultaneously, and all affecting drug absorption, distribution, elimination and excretion. The PBPK modelling approach provides an efficient methodology for incorporating such prior information within a Bayesian framework. For example, once developmental changes in organ size and compositions have been incorporated into the PBPK model, the possible accumulation of drug in a specific tissue can be predicted. Understanding changes in tissue drug concentrations is a key point in exploring the possibility of permanent adverse effects due to toxicity in a specific tissue. Thus, population PBPK models can help in different risk assessment applications, including screening chemicals for further testing, reverse dosimetry or estimating data-derived extrapolation factors [105].

5 Conclusions

Integrated system parameters for building a stochastic preterm PBPK model were compiled and incorporated within the Simcyp Simulator population library. These population data aim to mechanistically predict pharmacokinetics in the preterm population and to account for inter-individual variability at different PMA, GA or PNA when coupled with the in vitro-in vivo extrapolation approach. This approach will facilitate the investigation of drug exposure and any associated toxicity in different body organs and age-varying drug–drug interactions, and to inform the design of clinical studies in the preterm patient population. Future developments should expand the model to the very preterm populations.

Compliance with Ethical Standards

Conflict of interest Khaled Abduljalil, Xian Pan, Amita Pansari, Trevor N. Johnson and Masoud Jamei are full-time employees of Certara UK Limited, Simcyp Division. The activities of Certara are supported by a consortium of pharmaceutical companies.

References

1. World Health Organization. Preterm birth: key facts. 2018. http://www.who.int/news-room/fact-sheets/detail/preterm-birth. Accessed 14 Aug 2018.

2. Blencowe H, Cousens S, Oestergaard MZ, Chou D, Moller AB, Narwal R, et al. National, regional, and worldwide estimates of preterm birth rates in the year 2010 with time trends since 1990 for selected countries: a systematic analysis and implications. Lancet. 2012;379:2162–72.

3. Blencowe H, Cousens S, Chou D, Oestergaard M, Say L, Moller AB, et al. Born too soon: the global epidemiology of 15 million preterm births. Reprod Health. 2013;10(Suppl. 1):S2.

4. Boivin A, Luo ZC, Audibert F, Masse B, Lefebvre F, Tessier R, et al. Risk for preterm and very preterm delivery in women who were born preterm. Obstet Gynecol. 2015;125:1177–84.

5. Kenyon CF, Knoppert DC, Lee SK, Vandenberghe HM, Chance GW. Amikacin pharmacokinetics and suggested dosage modifications for the preterm infant. Antimicrob Agents Chemother. 1990;34:265–8.

6. Vandendriessche A, Allegaert K, Cossey V, Naulaers G, Saegeman V, Smits A. Prospective validation of neonatal vancomycin dosing regimens is urgently needed. Curr Ther Res Clin Exp. 2014;76:51–7.

7. Friis-Hansen B. Body water compartments in children: changes during growth and related changes in body composition. Pediatrics. 1961;28:169–81.

8. Fuchs A, Guidi M, Giannoni E, Werner D, Buclin T, Widmer N, et al. Population pharmacokinetic study of gentamicin in a large cohort of premature and term neonates. Br J Clin Pharmacol. 2014;78:1090–101.

9. Gonzalez D, Delmore P, Bloom BT, Cotten CM, Poindexter BB, McGowan E, et al. Clindamycin pharmacokinetics and safety in preterm and term infants. Antimicrob Agents Chemother. 2016;60:2888–94.

10. Aranda JV, Varvarigou A, Beharry K, Bansal R, Bardin C, Modanlou H, et al. Pharmacokinetics and protein binding of intravenous ibuprofen in the premature newborn infant. Acta Paediatr. 1997;86:289–93.

11. De Cock RF, Smits A, Allegaert K, de Hoon J, Saegeman V, Danhof M, et al. Population pharmacokinetic modelling of total and unbound cefazolin plasma concentrations as a guide for dosing in preterm and term neonates. J Antimicrob Chemother. 2014;69:1330–8.

12. Johnson TN, Rostami-Hodjegan A, Tucker GT. Prediction of the clearance of eleven drugs and associated variability in neonates, infants and children. Clin Pharmacokinet. 2006;45:931–56.

13. Templeton IE, Jones NS, Musib L. Pediatric dose selection and utility of PBPK in determining dose. AAPS J. 2018;20:31.

14. Shebley M, Sandhu P, Emami Riedmaier A, Jamei M, Narayanan R, Patel A, et al. Physiologically based pharmacokinetic model qualification and reporting procedures for regulatory submissions: a consortium perspective. Clin Pharmacol Ther. 2018;104:88–110.

15. Luzon E, Blake K, Cole S, Nordmark A, Versantvoort C, Berglund EG. Physiologically based pharmacokinetic modeling in regulatory decision-making at the European Medicines Agency. Clin Pharmacol Ther. 2017;102:98–105.

16. Wagner C, Zhao P, Pan Y, Hsu V, Grillo J, Huang SM, et al. Application of physiologically based pharmacokinetic (PBPK) modeling to support dose selection: report of an FDA Public Workshop on PBPK. CPT Pharmacometr Syst Pharmacol. 2015;4:226–30.

17. Abduljalil K, Pan X, Pansari A, Johnson TN, Jamei M. Preterm physiologically-based pharmacokinetic model. Part II: applications of the model to predict drugs pharmacokinetics in preterm population. Clin Pharmacokinet. **(in Press)**.

18. Royal College of Paediatrics and Child Health. UK-WHO growth chart-neonatal and infant close monitoring (NICM). 2009. https://www.rcpch.ac.uk/resources/uk-who-growth-charts-neonatal-infant-close-monitoring-nicm. Accessed 24 Sept 2019.

19. Abduljalil K, Jamei M, Johnson TN. Fetal Physiologically based pharmacokinetic models: systems information on the growth and composition of fetal organs. Clin Pharmacokinet. 2019;58:235–62.

20. Abduljalil K, Johnson TN, Rostami-Hodjegan A. Fetal physiologically-based pharmacokinetic models: systems information on fetal biometry and gross composition. Clin Pharmacokinet. 2018;57:1149–71.

21. Meban C. The surface area and volume of the human fetus. J Anat. 1983;137(Pt 2):271–8.

22. Rhodin MM, Anderson BJ, Peters AM, Coulthard MG, Wilkins B, Cole M, et al. Human renal function maturation: a quantitative description using weight and postmenstrual age. Pediatr Nephrol. 2009;24:67–76.

23. Abduljalil K, Jamei M, Rostami-Hodjegan A, Johnson TN. Changes in individual drug-independent system parameters during virtual paediatric pharmacokinetic trials: introducing time-varying physiology into a paediatric PBPK model. AAPS J. 2014;16:568–76.

24. Jamei M, Dickinson GL, Rostami-Hodjegan A. A framework for assessing inter-individual variability in pharmacokinetics using virtual human populations and integrating general knowledge of physical chemistry, biology, anatomy, physiology and genetics: a tale of 'bottom–up' vs 'top–down' recognition of covariates. Drug Metab Pharmacokinet. 2009;24:53–75.

25. Haycock GB, Schwartz GJ, Wisotsky DH. Geometric method for measuring body surface area: a height-weight formula validated in infants, children, and adults. J Pediatr. 1978;93:62–6.

26. Chemotherapy Standardisation Group (CCLG). Estimation of body-surface area in infants and children. 2008. https://www.ouh.nhs.uk/oxparc/professionals/documents/Body-surfaceareaCCLGChart1.pdf. Accessed 24 Sept 2019.

27. Paediatrica Acta. Total body water. Acta Paediatr. 1957;46:19–35.

28. Friis-Hansen B. Water distribution in the foetus and newborn infant. Acta Paediatr Scand Suppl. 1983;305:7–11.

29. Hytten F, Leitch I. The physiology of human pregnancy. 2nd ed. Oxford: Blackwell Scientific Publications Ltd; 1971.

30. Fomon SJ, Haschke F, Ziegler EE, Nelson SE. Body composition of reference children from birth to age 10 years. Am J Clin Nutr. 1982;35:1169–75.

31. Hartnoll G, Betremieux P, Modi N. Body water content of extremely preterm infants at birth. Arch Dis Child Fetal Neonatal Ed. 2000;83:F56–9.

32. Demarini S, Koo WW, Hockman EM. Bone, lean and fat mass of newborn twins versus singletons. Acta Paediatr. 2006;95:594–9.

33. Kelly HJ, Sloan RE, Hoffman W, Saunders C. Accumulation of nitrogen and six minerals in the human fetus during gestation. Hum Biol. 1951;23:61–74.

34. Anblagan D, Deshpande R, Jones NW, Costigan C, Bugg G, Raine-Fenning N, et al. Measurement of fetal fat in utero in normal and diabetic pregnancies using magnetic resonance imaging. Ultrasound Obstet Gynecol. 2013;42:335–40.

35. Enzi G, Zanardo V, Caretta F, Inelmen EM, Rubaltelli F. Intrauterine growth and adipose tissue development. Am J Clin Nutr. 1981;34:1785–90.

36. Friis CM, Qvigstad E, Paasche Roland MC, Godang K, Voldner N, Bollerslev J, et al. Newborn body fat: associations with maternal metabolic state and placental size. PLoS One. 2013;8:e57467.

37. Lampl M, Lee W, Koo W, Frongillo EA, Barker DJ, Romero R. Ethnic differences in the accumulation of fat and lean mass in late gestation. Am J Hum Biol. 2012;24:640–7.

38. Verkauskiene R, Beltrand J, Claris O, Chevenne D, Deghmoun S, Dorgeret S, et al. Impact of fetal growth restriction on body composition and hormonal status at birth in infants of small

and appropriate weight for gestational age. Eur J Endocrinol. 2007;157:605–12.

39. International Commission on Radiological Protection (ICRP). Basic anatomical and physiological data for use in radiological protection reference values. ICRP Publication 89. Ann ICRP. 2002;32(3–4).

40. Jopling J, Henry E, Wiedmeier SE, Christensen RD. Reference ranges for hematocrit and blood hemoglobin concentration during the neonatal period: data from a multihospital health care system. Pediatrics. 2009;123:e333–7.

41. Berrebi A, Benichou AC, Sarramon MF, Bessieres MH, Rolland M, Kobuch WE, et al. Biological reference values in the human fetus. 106 cord blood sampling in utero. J Gynecol Obstet Biol Reprod. 1992;21:355–9.

42. Boulot P, Cattaneo A, Taib J, Peray P, Lefort G, Hedon B, et al. Hematologic values of fetal blood obtained by means of cordocentesis. Fetal Diagn Ther. 1993;8:309–16.

43. Forestier F, Daffos F, Catherine N, Renard M, Andreux JP. Developmental hematopoiesis in normal human fetal blood. Blood. 1991;77:2360–3.

44. Wright IM, Goodall SR. Blood pressure and blood volume in preterm infants. Arch Dis Child Fetal Neonatal Ed. 1994;70:F230–1.

45. Bauer K, Linderkamp O, Versmold HT. Systolic blood pressure and blood volume in preterm infants. Arch Dis Child. 1993;69:521–2.

46. Leipala JA, Talme M, Viitala J, Turpeinen U, Fellman V. Blood volume assessment with hemoglobin subtype analysis in preterm infants. Biol Neonate. 2003;84:41–4.

47. Mollison PL, Veall N, Cutbush M. Red cell and plasma volume in newborn infants. Arch Dis Child. 1950;25:242–53.

48. Linderkamp O, Mader T, Butenandt O, Riegel KP. Plasma volume estimation in severely ill infants and children using a simplified Evans blue method. Eur J Pediatr. 1977;125:135–41.

49. McNamara PJ, Alcorn J. Protein binding predictions in infants. AAPS Pharmsci. 2002;4:E4.

50. Moniz CF, Nicolaides KH, Bamforth FJ, Rodeck CH. Normal reference ranges for biochemical substances relating to renal, hepatic, and bone function in fetal and maternal plasma throughout pregnancy. J Clin Pathol. 1985;38:468–72.

51. Krauer B, Dayer P, Anner R. Changes in serum albumin and alpha 1-acid glycoprotein concentrations during pregnancy: an analysis of fetal-maternal pairs. Br J Obstet Gynaecol. 1984;91:875–81.

52. Forestier F, Daffos F, Rainaut M, Bruneau M, Trivin F. Blood chemistry of normal human fetuses at midtrimester of pregnancy. Pediatr Res. 1987;21:579–83.

53. Gitlin D, Boesman M. Serum alpha-fetoprotein, albumin, and gamma-G-globulin in the human conceptus. J Clin Investig. 1966;45:1826–38.

54. Nau H, Krauer B. Serum protein binding of valproic acid in fetus-mother pairs throughout pregnancy: correlation with oxytocin administration and albumin and free fatty acid concentrations. J Clin Pharmacol. 1986;26:215–21.

55. Seta N, Tissot B, Forestier F, Feger J, Daffos F, Durand G. Changes in alpha 1-acid glycoprotein serum concentrations and glycoforms in the developing human fetus. Clin Chim Acta. 1991;203:167–75.

56. Belpaire FM, Wynant P, Van Trappen P, Dhont M, Verstraete A, Bogaert MG. Protein binding of propranolol and verapamil enantiomers in maternal and foetal serum. Br J Clin Pharmacol. 1995;39:190–3.

57. Bardy AH, Hiilesmaa VK, Teramo K, Neuvonen PJ. Protein binding of antiepileptic drugs during pregnancy, labor, and puerperium. Ther Drug Monit. 1990;12:40–6.

58. Poulin P, Theil FP. Development of a novel method for predicting human volume of distribution at steady-state of basic drugs

59. and comparative assessment with existing methods. J Pharm Sci. 2009;98:4941–61.

59. Berezhkovskiy LM. Determination of volume of distribution at steady state with complete consideration of the kinetics of protein and tissue binding in linear pharmacokinetics. J Pharm Sci. 2004;93:364–74.

60. Rodgers T, Rowland M. Mechanistic approaches to volume of distribution predictions: understanding the processes. Pharm Res. 2007;24:918–33.

61. White DR, Widdowson EM, Woodard HQ, Dickerson JW. The composition of body tissues (II). Fetus to young adult. Br J Radiol. 1991;64:149–59.

62. Dickerson JWT. Changes in the composition of the human femur during growth. Biochem J. 1962;82:56–61.

63. Fee BA, Weil WB Jr. Body composition of infants of diabetic mothers by direct analysis. Ann N Y Acad Sci. 1963;110:869–97.

64. Dobbing J, Sands J. Quantitative growth and development of human brain. Arch Dis Child. 1973;48:757–67.

65. Shah RS, Rajalakshmi R. Studies on human fetal tissues: II. Lipid composition of human fetal tissues in relation to gestational age, fetal size and maternal nutritional status. Indian J Pediatr. 1988;55:272–82.

66. Widdowson EM, Dickerson JW. The effect of growth and function on the chemical composition of soft tissues. Biochem J. 1960;77:30–43.

67. Iyengar L, Apte SV. Nutrient stores in human foetal livers. Br J Nutr. 1972;27:313–7.

68. Brans YW, Shannon DL. Chemical changes in human skeletal muscle during fetal development. Biol Neonate. 1981;40:21–8.

69. Dickerson JW, Widdowson EM. Chemical changes in skeletal muscle during development. Biochem J. 1960;74:247–57.

70. Agata Y, Hiraishi S, Oguchi K, Misawa H, Horiguchi Y, Fujino N, et al. Changes in left ventricular output from fetal to early neonatal life. J Pediatr. 1991;119:441–5.

71. Alverson DC, Eldridge MW, Johnson JD, Aldrich M, Angelus P, Berman W Jr. Noninvasive measurement of cardiac output in healthy preterm and term newborn infants. Am J Perinatol. 1984;1:148–51.

72. Aquilano G, Galletti S, Aceti A, Vitali F, Faldella G. Bi-level CPAP does not change central blood flow in preterm infants with respiratory distress syndrome. Ital J Pediatr. 2014;40:60.

73. Broadhouse KM, Finnemore AE, Price AN, Durighel G, Cox DJ, Edwards AD, et al. Cardiovascular magnetic resonance of cardiac function and myocardial mass in preterm infants: a preliminary study of the impact of patent ductus arteriosus. J Cardiovasc Magn Reson. 2014;16:54.

74. Evans N, Kluckow M. Early determinants of right and left ventricular output in ventilated preterm infants. Arch Dis Child Fetal Neonatal Ed. 1996;74:F88–94.

75. Ficial B, Finnemore AE, Cox DJ, Broadhouse KM, Price AN, Durighel G, et al. Validation study of the accuracy of echocardiographic measurements of systemic blood flow volume in newborn infants. J Am Soc Echocardiogr. 2013;26:1365–71.

76. Grollmuss O, Gonzalez P. Non-invasive cardiac output measurement in low and very low birth weight infants: a method comparison. Front Pediatr. 2014;2:16.

77. Laubscher B, van Melle G, Fawer CL, Sekarski N, Calame A. Haemodynamic changes during high frequency oscillation for respiratory distress syndrome. Arch Dis Child Fetal Neonatal Ed. 1996;74:F172–6.

78. Lindner W, Seidel M, Versmold HT, Dohlemann C, Riegel KP. Stroke volume and left ventricular output in preterm infants with patent ductus arteriosus. Pediatr Res. 1990;27:278–81.

79. Sinha AK, Cane C, Kempley ST. Blood flow in the common carotid artery in term and preterm infants: reproducibility and

relation to cardiac output. Arch Dis Child Fetal Neonatal Ed. 2006;91:F31–5.

80. Sloot SC, de Waal KA, van der Lee JH, van Kaam AH. Central blood flow measurements in stable preterm infants after the transitional period. Arch Dis Child Fetal Neonatal Ed. 2010;95:F369–72.

81. van Vonderen JJ, Roest AA, Siew ML, Blom NA, van Lith JM, Walther FJ, et al. Noninvasive measurements of hemodynamic transition directly after birth. Pediatr Res. 2014;75:448–52.

82. Victor S, Appleton RE, Beirne M, Marson AG, Weindling AM. The relationship between cardiac output, cerebral electrical activity, cerebral fractional oxygen extraction and peripheral blood flow in premature newborn infants. Pediatr Res. 2006;60:456–60.

83. Visser MO, Leighton JO, van de Bor M, Walther FJ. Renal blood flow in neonates: quantification with color flow and pulsed Doppler US. Radiology. 1992;183:441–4.

84. Walther FJ, Kim DH, Ebrahimi M, Siassi B. Pulsed Doppler measurement of left ventricular output as early predictor of symptomatic patent ductus arteriosus in very preterm infants. Biol Neonate. 1989;56:121–8.

85. Walther FJ, Siassi B, Ramadan NA, Ananda AK, Wu PY. Pulsed Doppler determinations of cardiac output in neonates: normal standards for clinical use. Pediatrics. 1985;76:829–33.

86. Winberg P, Ergander U. Relationship between heart rate, left ventricular output, and stroke volume in preterm infants during fluctuations in heart rate. Pediatr Res. 1992;31:117–20.

87. Yanowitz TD, Yao AC, Pettigrew KD, Werner JC, Oh W, Stonestreet BS. Postnatal hemodynamic changes in very-low-birth-weight infants. J Appl Physiol. 1985;1999(87):370–80.

88. Vieux R, Hascoet JM, Merdariu D, Fresson J, Guillemin F. Glomerular filtration rate reference values in very preterm infants. Pediatrics. 2010;125:e1186–92.

89. Desdicioglu K, Malas MA, Evcil EH. Development of the fetal duodenum: a postmortem study. Fetal Diagn Ther. 2009;26:16–23.

90. Touloukian RJ, Smith GJ. Normal intestinal length in preterm infants. J Pediatr Surg. 1983;18:720–3.

91. Rao-Mohandas KG, Somayaji SN, Bairy KL, Nayak S, Vincent R. A study to evaluate the relationship between the age of the fetus and intestinal length. Eur J Anat. 2006;10:151–2.

92. Johnson TN, Tanner MS, Taylor CJ, Tucker GT. Enterocytic CYP3A4 in a paediatric population: developmental changes and the effect of coeliac disease and cystic fibrosis. Br J Clin Pharmacol. 2001;51:451–60.

93. Fakhoury M, Litalien C, Medard Y, Cave H, Ezzahir N, Peuchmaur M, et al. Localization and mRNA expression of CYP3A and P-glycoprotein in human duodenum as a function of age. Drug Metab Dispos. 2005;33:1603–7.

94. Jamei M, Marciniak S, Feng K, Barnett A, Tucker G, Rostami-Hodjegan A. The Simcyp population-based ADME simulator. Expert Opin Drug Metab Toxicol. 2009;5:211–23.

95. Lacroix D, Sonnier M, Moncion A, Cheron G, Cresteil T. Expression of CYP3A in the human liver: evidence that the shift between CYP3A7 and CYP3A4 occurs immediately after birth. Eur J Biochem. 1997;247:625–34.

96. Stevens JC, Hines RN, Gu C, Koukouritaki SB, Manro JR, Tandler PJ, et al. Developmental expression of the major human hepatic CYP3A enzymes. J Pharmacol Exp Ther. 2003;307:573–82.

97. Hines RN. Ontogeny of human hepatic cytochromes P450. J Biochem Mol Toxicol. 2007;21:169–75.

98. Salem F, Johnson TN, Abduljalil K, Tucker GT, Rostami-Hodjegan A. A re-evaluation and validation of ontogeny functions for cytochrome P450 1A2 and 3A4 based on in vivo data. Clin Pharmacokinet. 2014;53:625–36.

99. Koukouritaki SB, Manro JR, Marsh SA, Stevens JC, Rettie AE, McCarver DG, et al. Developmental expression of human hepatic CYP2C9 and CYP2C19. J Pharmacol Exp Ther. 2004;308:965–74.

100. Treluyer JM, Jacqz-Aigrain E, Alvarez F, Cresteil T. Expression of CYP2D6 in developing human liver. Eur J Biochem. 1991;202:583–8.

101. Stevens JC, Marsh SA, Zaya MJ, Regina KJ, Divakaran K, Le M, et al. Developmental changes in human liver CYP2D6 expression. Drug Metab Dispos. 2008;36:1587–93.

102. Claassen K, Thelen K, Coboeken K, Gaub T, Lippert J, Allegaert K, et al. Development of a physiologically-based pharmacokinetic model for preterm neonates: evaluation with in vivo data. Curr Pharm Des. 2015;21:5688–98.

103. Yang X, Wu H, Mehta D, Sullivan MC, Wang J, Burckart GJ, et al. Ontogeny equations with probability distributions for anthropomorphic measurements in preterm and term neonates and infants for use in a PBPK model. Comput Toxicol. 2019;11:101–17.

104. Rostami-Hodjegan A, Tamai I, Pang KS. Physiologically based pharmacokinetic (PBPK) modeling: it is here to stay! Biopharm Drug Dispos. 2012;33:47–50.

105. Wetmore BA, Allen B, Clewell HJ 3rd, Parker T, Wambaugh JF, Almond LM, et al. Incorporating population variability and susceptible subpopulations into dosimetry for high-throughput toxicity testing. Toxicol Sci. 2014;142:210–24.